

# Micro Investigation into Positron Annihilation, Tribological and Mechanical Properties of Compacted Zn, ZnO<sub>2</sub> and Zn-ZSM-5 Nano Powders

Hala M. Abo-Dief

Associate Professor, Chemistry Dept., Faculty of Science, Al-Taif Univ., Al-Taif, KSA.  
On leave from The Egyptian Petroleum Research Institute Nasr City, Cairo, Egypt,

**Abstract:** *The application of Nanotechnology of metals has recently gained momentum, and environmental impact. Nano composites are known for their outstanding mechanical and physical properties due to their extremely fine grain size and high grain boundary volume fraction. The present work aimed at investigating the positron annihilation, tribological and mechanical properties of compacted Zn, ZnO<sub>2</sub> and Zn-ZSM-5 Nano Powders. The Nano specimens are compacted at constant compaction force of 130KN at room temperature. A wear test is carried out at a wear linear velocity range of 0.65 to 1.65 m/sec. The effect of both h/d and wear linear velocity on the compaction force, weight loss, compressive strength and Vicker's micro hardness are carried and investigated. The Nano compacted specimens of the optimum h/d ratio are heated at temperature range from 100°C to 400°C and used to discuss the effect of the compaction process and heating temperature on the number and size of the compaction voids of the Nano materials used. It is clear that as h/d decreases, both mechanical and tribological properties increases and as compacted Nano powders temperature increases, the void size increases and void numbers decreases. The Zn-ZSM-5 Nano compacted powders has higher tribological, mechanical and better positron annihilation properties compared to both Nano Zn and ZnO<sub>2</sub> compactions respectively.*

**Keywords:** Zn, ZnO<sub>2</sub> and Zn-ZSM-5 compacted Nano powders, compression and wear test, positron annihilation, and Vicker's micro hardness.

## 1. Introduction

Nanostructures are known for their outstanding mechanical and physical properties due to their extremely fine grain size and high grain boundary volume fraction. Significant progress has been made in various aspects of synthesis of Nano-scale materials. The focus is now shifting from synthesis to manufacture of useful structures and coatings having greater wear and corrosion resistance, [1]. Abo-Dief [2] concluded that Zn-ZSM-5 is non-permeable and their corrosion resistance is higher than pure Zn and ZnO coatings respectively. Abo-Dief et al., [3] deposited Nano zinc coatings on stainless steel by electro-deposition. The effect of Zn Nano particles on the morphology and corrosion properties is investigated. The results showed that addition of Nano Zn increases the corrosion resistance. Harishanand et al., [4] showed that Nano-particles represent appropriate wettability with metal at the time of sintering and good stability as well. While, Abdel Hameed et al., [5] concluded that Nano composites have also proven to be an effective alternative to other hazardous and toxic compounds. Altan et al., [6] illustrated that Nanotechnology is expected to make a significant contribution to the fields of computer storage, semiconductors, biotechnology, manufacturing, energy, chemical and coating industry. Mathiazhagan and Joseph, [7] produced Nano-sized particles and Nano scale system components that have new properties which are of importance for the development of new products and applications. Shahhoseyni, and Qods, [8] found that Nano-reinforcement in the matrix improved the initial bonding strength. Raju et al., [9] shown that the smaller is the particle, the higher is the surface-to-volume ratio. Chandran and Bapu, [10] found that zinc coatings by electro-deposition have extensive use for the corrosion protection of steel components.

Powder compaction is a popular route for the production of light engineering components such as automotive parts. Densification proceeds in two stages as follows; stage I, the microstructure can be idealized as discrete particles connected by necks at their contacts. This stage prevails up to a relative density of about 0.9. Stage II exists at higher relative densities and the microstructure comprises a distribution of interconnected or isolated voids. Mohamed et al., [11] studied the cold compaction of aluminum powder reinforced with copper wires. The effect of the height/diameter ratio of the compacted specimens on both the compressive strength and VHN is carried out and investigated. A comparison between the corrosion wear effect of the compacted and extruded specimens is introduced using; NaOH, HCl, H<sub>2</sub>SO<sub>4</sub> and HNO<sub>3</sub> as a corrosion mediums with a concentration of 1%, 5%, and 10% at a corrosion period of 10 min, 30 min and 60 min. Loto [12] examined the quality of electroplated zinc on mild steel in acid chloride solution at ambient temperature. The surface of the plated steel was examined with scanning electron microscopy, and energy dispersive spectroscopy. Sophia et al., [13] synthesized intrinsically conducting polymer metal Nano composites by polymerizing anthranilic acid (PANA) with ferric chloride, Zinc oxide and Magnesium oxide by chemical oxidation method.

Safaei et al., [14] proved that coating that has a reasonable cost protection and exhibits sufficient air resistance. These properties make zinc a proper coating material. Penkov et al., [15] evaluated the tribological behavior of carbon-zinc oxide composite coatings (CZnO) using an atmospheric pressure plasma jet method with a reciprocating pin-on-disk tribo-tester. The results showed that the frictional behavior and the wear resistance of the ZnO coating could be significantly improved with the addition of carbon. Al-

Ghamdi et al., [16] investigated both the frictional behavior and the effect of sliding mode of woven fabrics and also discussed the effect of sliding modes and mediums on the electrostatic charge and corrosivity of epoxy/aluminium reinforced composites [17]. Bellemare et al., [18] deduced that material hardness have been used extensively for material characterization and also as a basis for predicting the tribological response. Petrik [19] used the Vicker's test for the determination of hardness of small items or thin layers. Firdous et al., [20] presented the results of indentation induced Vicker's micro hardness and fracture toughness in the load range of 0.049 to 3N on pure Ni modified ZnS Nano crystals. Al-Ghamdi et al., [21] discussed the reinforced epoxy composites characteristics. Mohamed et al., [22] discussed the positron annihilation lifetime of compacted iron powder and El-Sayed et al., [23] compared the positron annihilation lifetimes with the mechanical properties of nickel-chromium. The ortho-positronium lifetime increases from 45 to 2.55 ns with compaction load increment from 30 to 50 tons. The result showed that there is direct correlation between the voids size and numbers with the load decrement. Xie et al., [24] established the positron annihilation spectroscopy (PAS) technique to study the materials defects. The present work is aimed at investigating the positron annihilation, tribological and mechanical properties of compacted Zn, ZnO<sub>2</sub> and Zn-ZSM-5 Nano Powders. The Nano specimens are compacted at constant compaction pressure of 130KN at room temperature. A wear test is carried out at a wear linear velocity range of 0.65 to 1.65 m/sec. The effect of both h/d ratio and wear linear velocity on the compaction force, weight loss, compressive strength and Vicker's micro hardness are carried and investigated. The effect of the type of the heated compacted specimens at h/d=0.5 at temperature range from 100<sup>o</sup>C to 400<sup>o</sup>C on the number and size of the voids of the three Nano materials are investigated using the positron annihilation method.

## 2. Experimental

### 2.1 Materials and Specimens

The Nano zinc, ZnO<sub>2</sub> and zinc composite (Zn-ZSM-5) metal powder with a mean size of 100 nm supplied by ADWIC is used for all specimens. Powder is weighted to the required weight using a balance (Metler H80, with an accuracy of 1 mg division). The cold powder compaction technique is used to produce cylindrical compacts of about 20gm weight and 24 mm diameter.

### 2.2 Compaction Process

A vertical press of 200 tons capacity is used. The load is directly read on the press graduated scale, while the punch travel is measured using a dial gauge settled against the moving press platen. Each type of the powders are first blended and fed into the mold, then closed by a dummy block, which is placed between the powder and the punch. The effect of specimen height/diameter (h/d) ratio is investigated at various test conditions. The present powder compaction technique is used to produce cylindrical compacts of about 12, 18, 24 and 36 mm height by pressing the powders under compaction loads up to 130KN. A

compaction set-up of sub-press is designed and manufactured for this purpose.

A universal testing machine was used for the compression experiments. Cross head speed was 5 mm/min for all experiments. Load values were recorded from load indicator, while displacement measurements were taken using a dial gage fixed against the moving platen of the machine. Two hardened steel flat platens were used. No lubrication was applied to the platen/specimen surfaces in all compression experiments. Experiments were continued until the beginning of fracture.

### 2.3 Wear test

The test is carried out using Pin-on-Disc wear device. It consists of a rotary horizontal steel disc driven by variable speed motor. The test specimen is held in the specimen holder that fastened to the loading lever against the rough counter face through two thin spring steel sheets. The load is applied by dead weights (1600gm) at six variable linear velocities ranges from 0.65 to 1.65 m/sec. The contact surface of the test specimens was polished by an emery paper before the test. The Pin-on-Disc counter face contained an emery paper of 80 grit attached to a steel disc of 50 mm inner diameter and 100 mm outer diameter and 2mm thickness.

### 2.4 Hardness Measurements

Micro hardness was tested using Vickers Micro-hardness tester with diamond indenter in the form of right pyramid and a square base. An optical microscope with up to 400X magnification along with a Micrometer attachment in the eye piece was used to observe and measure the length of the diagonal of indentation. Bulk hardness measurements were carried out using a standard CARL-ZEISS Vicker's hardness tester. Hardness variations in the subsurface regions were monitored by making indentations on the transverse sections. A total of three indentations were made at a particular depth and the mean value was taken.

### 2.5 Microscopy

After the abrasion testing, the samples were sectioned perpendicularly to the abraded surface of 1.3X1.3X1.1 cm, mounted in cold-setting polyester resin, sputter with gold and examined by SEM of the Minia University central laboratory to study the abrasion-induced microstructure changes in regions closed to the abraded surface.

### 2.6 Positron Annihilation Test

The method is based on the fact that positron lifetime increases with defects increment due to low electron density. It is a technique in which the positrons energetic beam is injected into a material where they rapidly diffuse in the material until they annihilate with an electron typically after 200 ps giving off a pair of 511 KeV photons. Positrons are generally trapped at open defects such as vacancies or small voids and thus positron annihilation spectroscopy can be used to determine the distribution of such defects in the bulk materials. The <sup>22</sup>Na

positron source held in a Kapton foil (activity of 20 Ci) sandwiched between two identical pieces of sample under investigation. The 1.275 MeV-ray from the decay of  $^{22}\text{Na}$  isotope is taken as the start signal, whereas one of the 0.511 MeV-rays from the positron annihilation in the studied material is the stop signal. Thus, the time interval between the above two-rays is the lifetime of the positron in the material. The lifetime spectra were analyzed using the PATFIT program with source corrections. Ps has two states due to their different spin, an anti-parallel spin state is called para-positronium (p-Ps), and a parallel spin state is called ortho-positronium (o-Ps). The o-Ps lifetime correlates to the free-volume hole size while the intensity of this o-Ps component contains information about the free-volume concentration. It is accustomed to fit PAL spectra into three lifetimes. The shortest-lived component (S1) with intensity (I1) is attributed to the annihilation of p-Ps and Ps-molecular species. The intermediate-lived component lifetime (S2) and intensity (I2) is attributed to the direct annihilation of positrons and positron-molecular species. The long-lived component with lifetime (S3) and intensity (I3) is o-Ps annihilation in free volume holes. The value of (S3) is sensitively depends on the changes of the free-volumes.

### 3. Results and Discussions

#### 3.1 Effect of H/D Relation

Figure 1 shows the effect of the (h/d) ratio on the compaction load/displacement relation. It is clear that as the ratio increases, the displacement increases. The inter-particles friction and interface distance between particles increase with increasing the amount of powder and that needs extra load to overcome. Also, as h/d decreases, the displacement decreases. In general, it is observed that there are three stages through the compaction stroke for all compaction load/displacement relation. In the first stage, powder particles are restacked or rearranged so that bridging, which occurs in a randomly arranged stack of loose powder particles, is partially eliminated and the deformation force tries to overcome frictional forces on the contacting surfaces and between grains, it is characterized by a rapid increase in the punch travel for relatively small loads. The second stage starts when the compression and compaction occur at the same time, the spaces between particles are decreased and the particle shape begins to change to fill the small spaces, it involves elastic and plastic deformation of the particles. The amount of plastic deformation depends on the ductility of the powder materials. At the third stage, the compaction begins to gain relatively high density, after which its resistance for forming increases, the powder particles fracture under the applied load and form smaller fragments. It is marked by a rapid increase in the punch load because of the required force to deform the particles must be high particularly when the billet density is nearly the full density. Furthermore, the mechanisms for the development of green strength during compaction are generated by two phenomena namely (i) particle sliding and interlocking and (ii) plastic deformation. It is clear that there is particles welding due to compaction pressure and forged (splayed) particles. The figure shows

that h/d=0.5 have lower displacement and higher strength followed by h/d= 0.75, 1.0 and 1.5 respectively.

#### 3.2 Compressive Strength

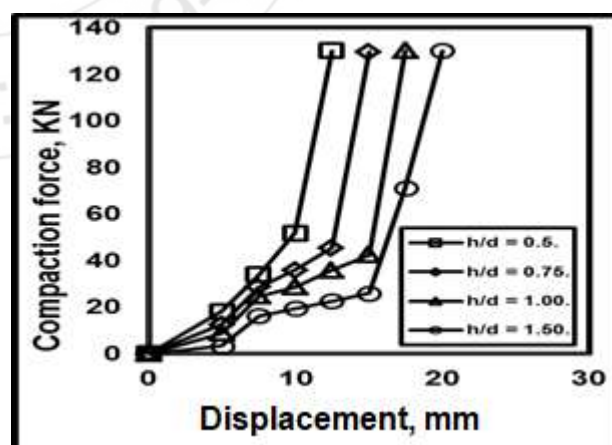
The compressive strength of the Nano zinc,  $\text{ZnO}_2$  and zinc composite (Zn-ZSM-5) was measured through compression test, which was carried out at room temperature. The strength of the compacted specimens that have h/d ratio equal 0.5 is the greatest, which confirm the previous explanation, as shown in Fig. 2. This is attributed to the strain hardening occurs in the specimens compacted that leads to the compressive strength increment.

#### 3.3 Vicker's Micro-Hardness

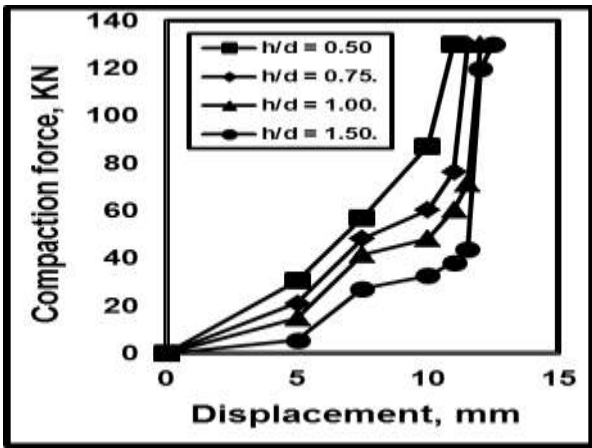
Hardness of a material is defined as the resistance to deformation, particularly permanent deformation, indentation or scratching. Results of Vicker's micro hardness test that carried out on the compacted specimens are shown in Fig.3, illustrates that increasing h/d ratio decreases the (VHN), this is due to the corresponding decrease in the compact density and porosity increment that means decreasing densification and bonding. So, as the h/d ratio decreases, the densification, strength and hardness of the Nano zinc,  $\text{ZnO}_2$  and zinc composite (Zn-ZSM-5) increases. Fig.11. shows representative micrographs of indentation marks.

#### 3.4 Wear Test

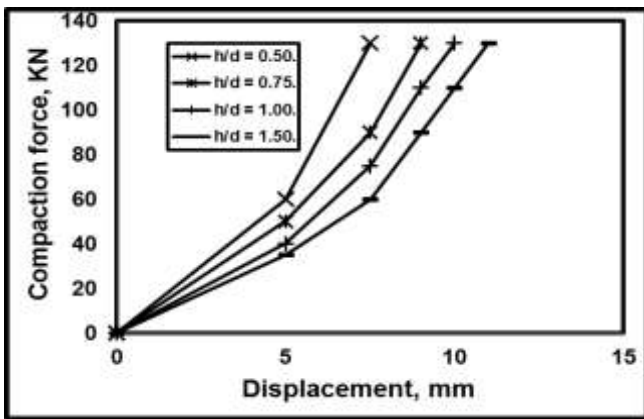
The evaluation of the compacted samples wear resistance is carried out on the basis of mass loss method and displayed in Fig.4. Sliding against metal counter face exhibits two main mechanisms, abrasion and adhesion. The process of building up a thin film goes from one stage to another until steady state is reached. Initially, the process begins with abrasion by which loose wear particles are produced and retained within the interface till their attachment or escape.



(1.a) Nano zinc



(1.b) Nano zinc oxide.



(1.c) Nano zinc composite.

Figure 1: Variation of compaction force/displacement at various height/diameter ratio

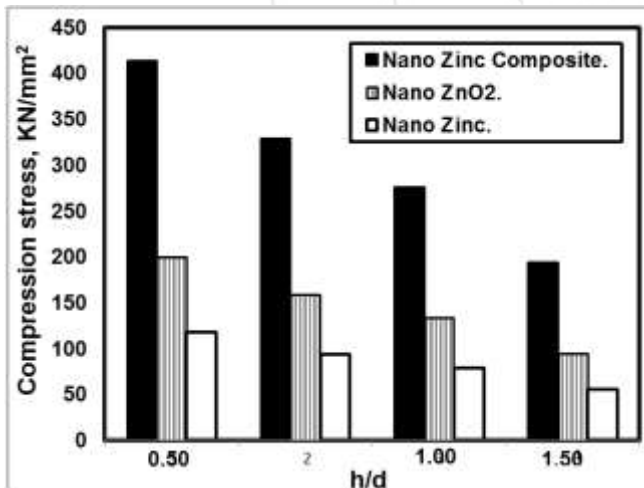


Figure 2: Effect of h/d ratio on the compressive strength of Nano zinc, ZnO<sub>2</sub> and zinc composite (Zn-ZSM-5) compacted powder.

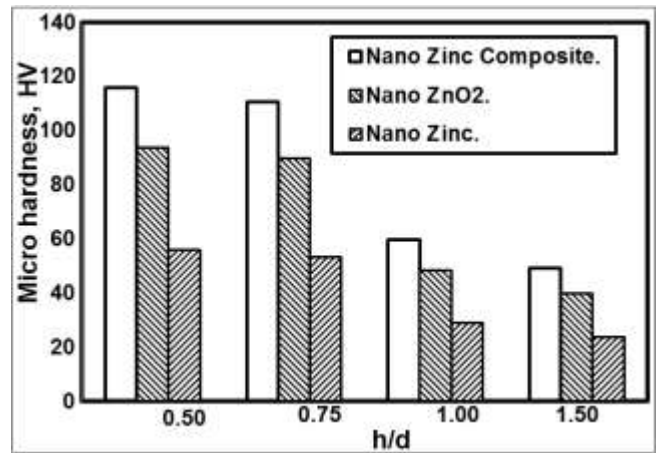
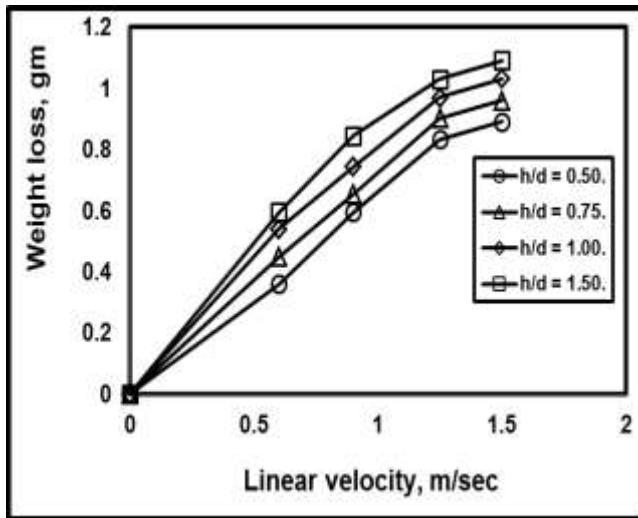


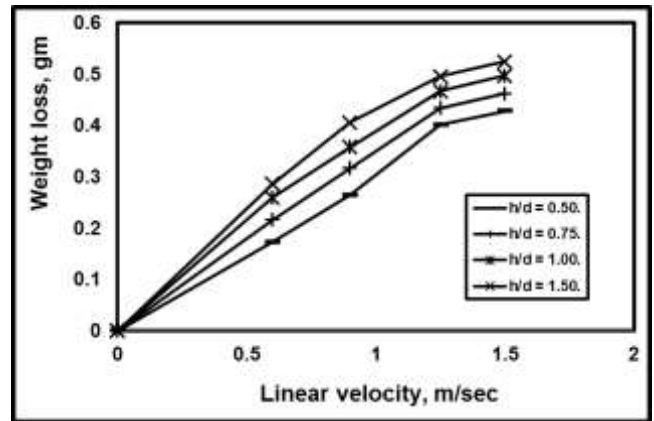
Figure 3: Effect of h/d ratio on the Vicker's micro hardness

The attached particles fill in the valleys of surface topography and as wear continues, the effectiveness of abrasion is reduced and a thin film is formed on the metal surface by adhesion, called "transfer film". After this stage, another thin film is simultaneously developed on the composite pin or back transferred from counter face into the composite pin, in either case is called "back transferred film". With increasing the wear linear sliding velocity, the specimen metal removal increases and the wear resistance decreases. As the h/d ratio decreases, the wear rate decreases because of the density increment that improves the welding and the powder compatibility. It can be seen that the wear rate increases at lower rate at early stages. When the test is increased, the wear rate increased rapidly due to the depth increment and the hardness increment. The wear rate decreased by decreasing the wear sliding velocity, and h/d ratio due to the hardness increment and the higher bonding of the greater areas between particles and the density increment. As the rotating speed increases, the wear resistance decreases due to the temperature increment and material softening. Also, as the h/d ratio decreases, the wear rate decreases because of the compatibility increment. For the same velocity it is clear that decreasing h/d ratio increases wear resistant (less weight loss).

The wear behaviors of the compacted specimens were observed using a SEM as shown in Fig. 5. Nano ZnO showed evidence of severe wear compared to Zn composite. A significant portion of the material was displaced from the center region of the wear track, forming burrs along the sides of the track. On the other hand, a wear track was formed on the Nano zinc composite, only a burnishing type of wear was detected. The wear surface shows a relatively flat morphology. In the second part of the wear surface, the rougher area is present with deeply eroded regions between Nano zinc composites. The particles wear proceeds by intergranular brittle fracture and the most wear resistant is at h/d=0.5, Fig. 5.a and 5.b. Fig. 5.c shows the result of smearing, and the formation of peaks, which are subsequently flattened. Fig. 5.d highlights the high density of plastic deformation accumulated at the edges of the flattened layers, resulted in material removal by chipping.

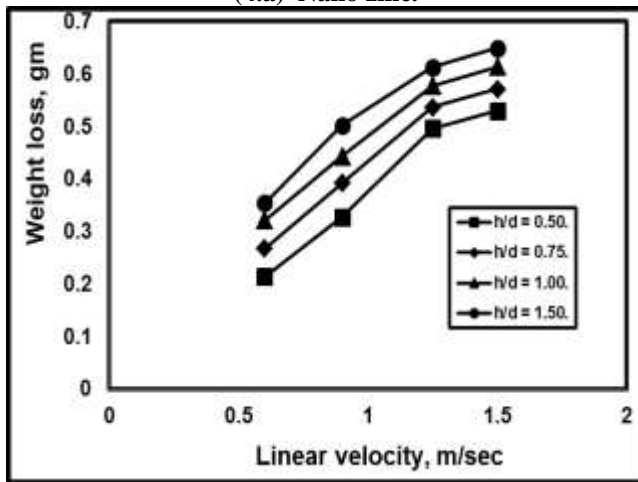


(4.a) Nano zinc.



(4.c) Nano zinc composite.

Figure 4: Effect of wear linear velocity on the compressive strength of Nano zinc, ZnO<sub>2</sub> and zinc composite (Zn-ZSM-5) compacted powder.



(4.b) Nano zinc oxide.

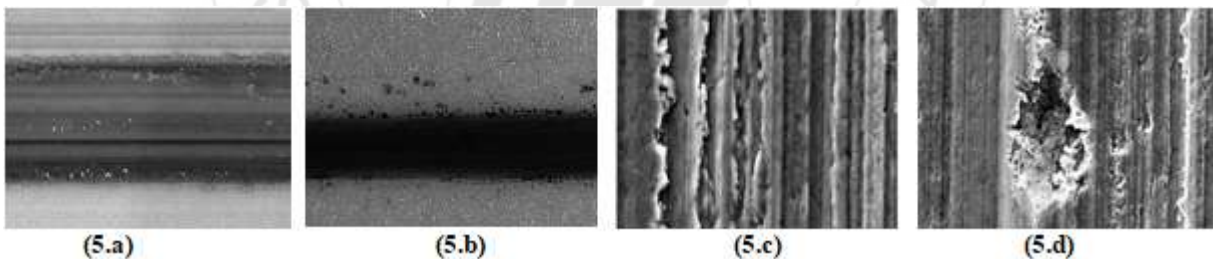


Figure 5: SEM images of the wear tracks and the worn surface.

(a) Nano ZnO, (b) Nano Zn composites, (c) Primary layer after sliding wear test, and (d) after sliding wear test.

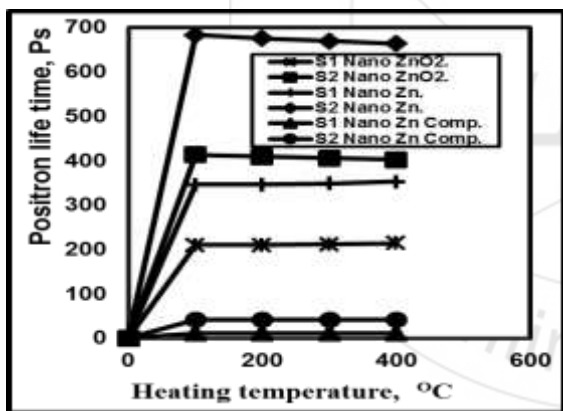
### 3.4. Positron annihilation

Considering the analysis of the positron lifetime spectra, all positrons injected into the compacted Nano zinc, ZnO<sub>2</sub> and zinc composite (Zn-ZSM-5) specimens are annihilated with lifetimes clearly longer than in the bulk zinc crystal (106 ps). Thus, all positrons are localized at traps before annihilation. In this case of saturation trapping, a general comparison of the positron lifetime in compacted Nano zinc, ZnO<sub>2</sub> and zinc composite (Zn-ZSM-5) powder at different compaction temperatures is given in Fig. 6-8. Figure 6.a and Figure 6.b show three positron lifetime components, S1, S2, and S3. It was reported that defect-free ZnO single crystal exhibited a single lifetime components of about 183 ps [25]. However, all specimens exhibit three lifetime components: a short lifetime S1, an intermediate lifetime S2 and a very long

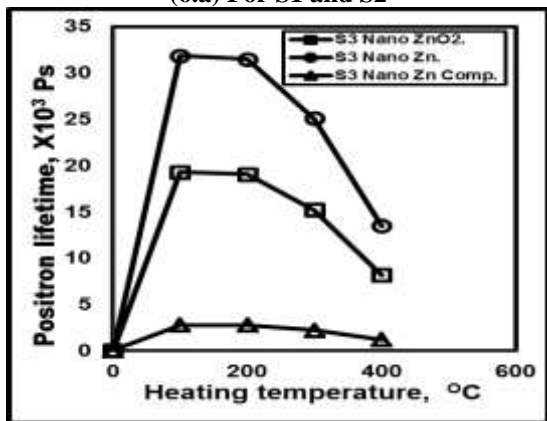
lifetime S3. This result indicates the existence of defects. (S3) is probably due to the annihilation of ortho-positronium atoms formed in the large voids which is the unoccupied space among close packed Nano particles. (S1) is generally attributed to the free annihilation of positrons in defect-free crystal. However, in disordered systems, smaller vacancies (like mono vacancies) decrease the average electron density, thus resulting in elongation of S1. In the present case, the larger S1 for the samples than that of the reported for Zn and ZnO single crystal suggests the presence of the mono vacancies in the samples, which may exist inside the grain or exist in the grain boundary region. The intermediate lifetime component (S2) is much larger than that of the mono vacancies (S1). This indicates that S2 arises from positrons trapped by larger size defects (e.g. Zn vacancy clusters) [25], since in such larger size defects, the average electron density

is lower than that in small size defects, thus decreasing the annihilation rate, and consequently increasing the positron lifetime [26]. These vacancy clusters usually locate at the grain surface and interface region [25]. As shown in Fig. 6.a, Nano Zn composite exhibits almost same S1 and S2, suggesting the presence of smaller size of defects compared to both Nano ZnO and Nano Zn samples respectively.

Besides the lifetime of the positron, its relative intensity (I) provides information on the relative concentration of the defects is shown in Fig. 7. The ratio of I<sub>2</sub>-I<sub>1</sub> (I<sub>2</sub>/I<sub>1</sub>) for Zn composite is 0.478, indicating that the concentration of small size mono vacancies in bulk or grain boundary is larger than that of larger size vacancy clusters at the grain surface and interface region. ZnO<sub>2</sub> and Zn exhibit a higher ratio of I<sub>2</sub>-I<sub>1</sub> (I<sub>2</sub>/I<sub>1</sub> = 0.7 and 0.76) respectively, indicating that the concentration of small size mono vacancies is almost same as that of larger size vacancy clusters for both Zn and ZnO<sub>2</sub>. The higher compaction temperature increases the interfacial area and thereby the overall density of vacancy-size traps up to 200°C followed by I<sub>3</sub> decrement. The size of voids may influence the long-time constant (I<sub>3</sub>) via the collision rate of the Ps atoms with the wall. On the other hand, as the compaction temperature increases than 200°C, I<sub>1</sub> increases, and both I<sub>2</sub> and I<sub>3</sub> decreases, this means that the size of the voids increases and the number of voids decreases by increasing the compaction temperature. From Figure 8, a decrement of the intensity ratio (I<sub>1</sub>/I<sub>2</sub>) appears to occur with temperature increment. This declares the effect of temperature on changing of o-Ps to p-Ps which decreases the compacts density and strength.

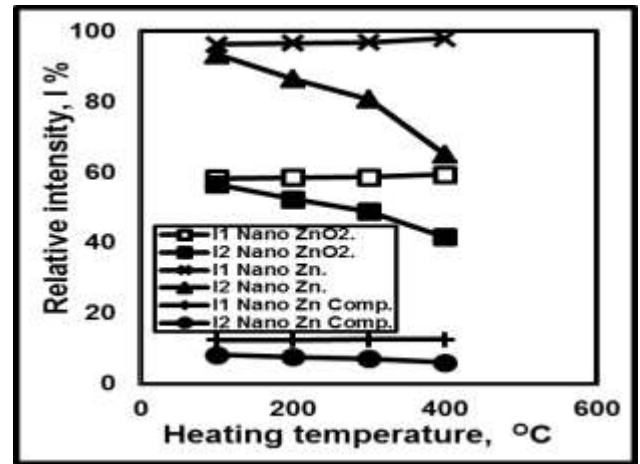


(6.a) For S1 and S2

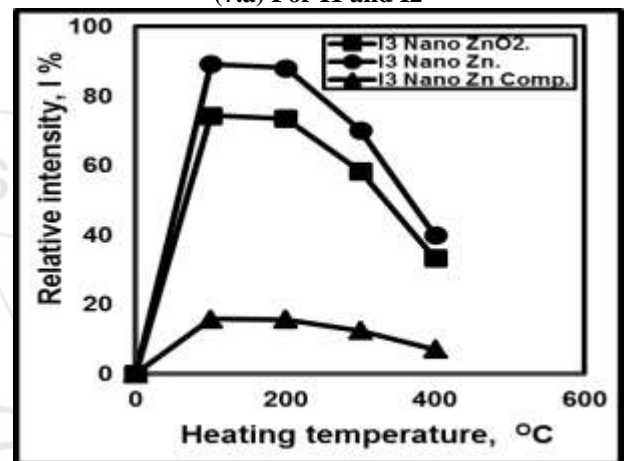


(6.b) For S3

Figure 6: Variation of positron lifetime (S1&S2) and positron lifetime S3.



(7.a) For I1 and I2



(7.b) For I3

Figure 7: Variation of positron intensity (I1&I2) and positron intensity I3.

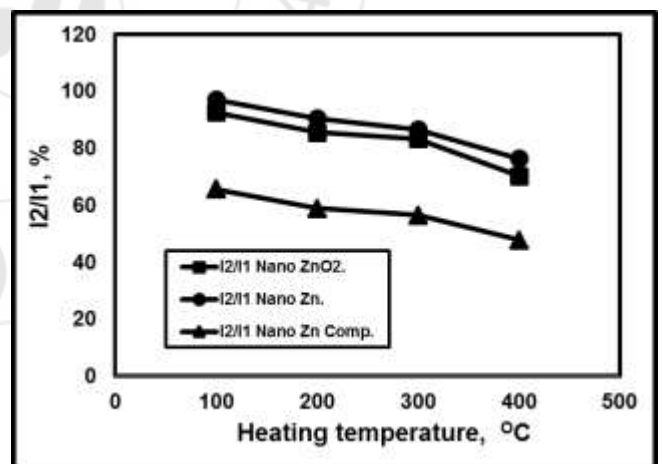


Figure 8: Variation of I2/I1 with heating temperature

#### 4. Conclusions

- 1) The powder metallurgy is a suitable technique for fabricating the Nano zinc, ZnO<sub>2</sub> and zinc composites (Zn-ZSM-5) at room temperatures.
- 2) As the compaction h/d ratio increases, both the compacted product density and soundness decreases.
- 3) The positron annihilation lifetime technique is found applicable in studying the material properties.
- 4) The number of voids that related to the o-Ps intensity decreases with increasing the compaction temperature

condition due to the aggregation of these voids that increases the void size.

- 5) The wear rate increases with increasing the wear linear velocity. Also the wear decreases with decreasing the compaction h/d ratio.
- 6) Both the hardness and the compression strength increases with decreasing the compaction h/d ratio.

## References

- [1] H.M. Abo-Dief, S.M.I. Morsi, and A.T. Mohamed, "Corrosion Inhibition using Deposited Nanoparticles", *Int. J. of Adv. Scientific and Technical Research*, I. 3 V. 6, pp. 787-797, Nov.-Dec. 2013.
- [2] H.M. Abo-Dief, "OCP and CCP Techniques of Nano Crystalline Zn, ZnO and Zn-ZSM-5 Coatings at H<sub>2</sub>S Corrosion Media", *Int. J. of Adv. Scien. and Techn. Res.*, Issue 4, V. 4, pp. 88-102, July-Aug. 2014.
- [3] H.M. Abo-Dief, S.A. Al-Ghamdi, E.S. Al-Zahrani and A.T. Mohamed, "Electro Deposition and Corrosion Properties Of Nano Coated Stainless Steel", *The 17<sup>th</sup> Int. Conf. on Advances and Trends in Eng. Mat. & their Applications*, Montreal, CANADA, pp. 201-211, June 16-20, 2014.
- [4] K.S. Harishanand, S. Datta, Dr. B.M. Nagabhushana, H. Nagabhushana, and M.M. Benal, "Mechanical properties and Corrosion Resistance of nano-Ceria doped Aluminium", *Int. J. of Eng. Research and Applications*, Vol. 2, Issue 5, pp.1030-1035, September- October 2012.
- [5] R.S. Abdel Hameed, A.H. Abu-Nawwas and H.A. Shehataa, "Nano-composite as corrosion inhibitors for steel alloys in different corrosive media", *Advances in Applied Science Research*, 4(3), pp. 126-129, 2013.
- [6] M. Altan, H. Yildirim and A. Uysal, "Tensile Properties of polypropylene/ Metal Oxide Nano Composites", *The Online Journal of Science and Technology*, V. 1, Iss. 1, pp. 26-30, Jan. 2011.
- [7] A. Mathiazhagan and R. Joseph, "Nanotechnology-A New Prospective in Organic Coating - Review", *Int. J. of Chemical Eng. and Applications*, Vol. 2, No. 4, pp. 225-237, Aug. 2011.
- [8] M. Shahhoseyni, and F. Qods, "Investigation of microstructure and mechanical properties of Cu/ZnO Nano composite produced by ARB process", *Mat. Scie. and Eng.*, 63, pp. 1-8, 2014.
- [9] B. Raju, K. Ramji and V. Prasad, "Studies On Tribological Properties of ZnO Filled Polymer Nanocomposites", *ARN J. of Eng. and Applied Scie.*, Vol. 6, No. 6, pp. 75-82, JUNE 2011.
- [10] M. Chandran and G.R. Babu, "Electrodeposition of Nano Zinc - Nickel Alloy from Bromide Based Electrolyte", *Research Journal of Chemical Sciences*, Vol. 3(8), 57-62, August 2013.
- [11] Ashraf T. Mohamed, Fahd A. Al-Zahrani, and H.M. Abo-Dief, "Conventional Extrusion Modeling Of Compacted Al/Cu Composites", *The Seventh Asian-Australian Conf. on Composite Materials (ACCM7)*, Taipei, Taiwan, November 15-18, 2010.
- [12] C.A. Loto, "Synergism Of Saccharum Officinatum And Ananas Comosus Extract Additives On The Quality Of Electroplated Zinc On Mild Steel", *Res Chem Intermed*, pp. 1-17, Feb. 2013.
- [13] I.A. Sophia, G. Gopu, and C. Vedhi, "Synthesis and Characterization of Poly Anthranilic Acid Metal Nano composites", *Open J. of Synthesis Theory and Applications*, 1, pp. 1-8, 2012.
- [14] H.R. Safaei, M.R. Safaei and V. Rahmanian, "Film Formation and Anticorrosive Behavior of Zn-ZSM-5 Nano-Sized Zeolite Composite Coatings", *Open Electrochem. J.*, pp. 1-8, 2012.
- [15] O. Penkov, D. Lee, H. Kim, and D. Kim, "Frictional behavior of atmospheric plasma jet deposited carbon-ZnO composite coatings", *Composites Scie. and Techn.*, 77, pp. 60-66, 2013.
- [16] S. Al-Ghamdi, H. Abo-Dief and A.T. Mohamed, "Investigation of Dielectric Properties and Frictional Behavior of Woven Fabrics", *The 17<sup>th</sup> Int. Conf. on Advances and Trends in Eng. Mat. and their Applications*, Montreal, CANADA, pp. 213-222, June 16-20, 2014.
- [17] S.A. Al-Ghamdi, F.A. Al-Zahrani, H.M. Abo-Dief, and A.T. Mohd., "Effect of Sliding Mode and Medium on The Electrostatic Charge and Corrosivity of Epoxy /Aluminium Reinforced Composites", *The 13<sup>th</sup> Int. Conf. "Advances and Trends in Eng. Mat. and their Applications"*, Montreal, CANADA, pp. 51-60, June 03-07, 2013.
- [18] S.C. Bellemare, M. Dao, and S. Suresh, "Effects of mechanical properties and surface friction on elastoplastic sliding contact", *Mechanics of Materials*, 40, pp. 206-219, 2008.
- [19] J. Petrik, "The Influence Of The Load on The Quality of Micro hardness Measurement", *Acta Metallurgica Slovaca*, Vol. 17, No. 3, p. 207-216, 2011.
- [20] A. Firdous, T. Rasool, G.N. Dar, and M.M. Ahmad, "Micro-Mechanical Studies On Pure And Ni Doped Zn Nanostructured Crystals", *Journal of Optoelectronics And Biomedical Materials* Vol. 2, Issue 4, Pp. 175-184. October-December 2010.
- [21] S.A. Al-Ghamdi, F.A. Al-Zahrani, H. M. Abo-Dief and A. T. Mohd. "Reinforced Epoxy Composites Characteristics", *Journal of American Scie.*; 9(3), pp. 297-303, 2013.
- [22] Ali M. El - Sayed, Ashraf T. Mohamed, and Esam E. Abdel-Hady, "Positron Annihilation Lifetimes in Comparison with The Mechanical Properties in Nickel-Chromium Alloy", *The 11<sup>th</sup> Int. Conf. on Positron Annihilation*, Kansas City, USA, pp. 55-57, May 25-30, 1997.
- [23] A.T. Mohamed, A.M.A. El-Sayed and H.F.M. Mohamed, "Positron Annihilation Lifetime in Compacted Iron Powder", *The Int. Conference on Nuclear and Particle Physics NUPPAC'97*, Nuclear Research Center, Atomic Energy Authority, Cairo, Egypt, pp. 22-26 Nov. 8-10, 1997.
- [24] W. Xie, Y. Li, W. Shi, L. Zhao, X. Zhao, P. Fang, F. Zheng, and S. Wang, "Novel effect of significant enhancement of gas-phase photocatalytic efficiency for Nano ZnO", *Chemical Engineering Journal*, 213, pp. 218-224, 2012.